Development 125, 293-300 (1998)
Printed in Great Britain © The Company of Biologists Limited 1998
DEV3755

Sperm-induced local $[Ca^{2+}]_i$ rise separated from the Ca^{2+} wave in sea urchin eggs in the presence of a gamete fusion inhibitor, jaspisin

Tatsuma Mohri[1,*], Shunichi Miyazaki[1,2], Hideki Shirakawa[2] and Susumu Ikegami[3]

[1]Laboratory of Intracellular Metabolism, Department of Molecular Physiology, National Institute for Physiological Sciences, Myodaiji-cho, Okazaki, 444, Japan
[2]Department of Physiology, Tokyo Women's Medical College, Shinjuku-ku, Tokyo, 162, Japan,
[3]Department of Applied Biochemistry, Hiroshima University, Higashi-hiroshima, 739, Japan
*Author for correspondence (e-mail: tsmohri@nips.ac.jp)

(Accepted 10 November 1997; published on WWW 1997)

SUMMARY

An increase in intracellular Ca^{2+} concentration ($[Ca^{2+}]_i$) at a focal plane was recorded simultaneously with sperm-egg binding and membrane current upon insemination of sea urchin *Hemicentrotus pulcherrimus* eggs. No change in current and $[Ca^{2+}]_i$ occurred in the presence of jaspisin, a novel substance that inhibits metallo-endoproteinase and sperm-egg membrane fusion (S. Ikegami, H. Kobayashi, Y. Myotoishi, S. Ohta and K. H. Kato (1994) *J. Biol. Chem.* 269, 23262-23267). With low doses of jaspisin, a spermatozoon first produced a step inward current (I_{on}) as an indication of gamete membrane fusion and then induced a local $[Ca^{2+}]_i$ rise at the site of sperm attachment 6-10 seconds after I_{on}. The sperm, however, soon detached from the egg. Increasing inward current was abruptly cut off (I_{off}) within 9-15 seconds and the local $[Ca^{2+}]_i$ rise began to decline 1-3 seconds after I_{off}. In most cases, no further responses or an elevation of fertilization envelope (FE) occurred. In some cases, $[Ca^{2+}]_i$ at the sperm attachment site increased again even after the sperm detached and triggered a Ca^{2+} wave which caused an activation current and FE formation. This recording of a gamete membrane-fusion-induced local $[Ca^{2+}]_i$ rise, separated from the Ca^{2+} wave, is a key phenomenon for elucidating the initial sperm stimulation of the egg at fertilization.

Key words: Fertilization, Sea urchin egg, Sperm-egg fusion, Jaspisin, Intracellular calcium, Calcium wave, Activation current

INTRODUCTION

The early events that occur in eggs at fertilization are the activation (or fertilization) potential and a dramatic increase in intracellular Ca^{2+} concentration ($[Ca^{2+}]_i$). Analyses of these events are of great significance in elucidating the mechanism by which sperm first stimulate the egg. The activation current under voltage clamp (the counterpart of the activation potential) has been analyzed in detail in the sea urchin *Lytechinus variegatus* egg (Lynn et al., 1988; Chambers, 1989). It comprises three phases: phase 1, an abrupt onset and slow increase of inward current to the maximum shoulder, phase 2, a more rapid increase to the major peak and phase 3, a rapid decline followed by a much slower decline. During phase 2, the fertilization envelope (FE) is elevated in a wave starting from the site of sperm attachment and spreading in the egg surface toward the antipode (Lynn et al., 1988), as a result of exocytotic secretion from cortical granules (Epel, 1978).

The increase in $[Ca^{2+}]_i$, which is a pivotal signal in egg activation, takes the form of a wave starting from the sperm attachment site and propagating across the egg (Jaffe, 1985). In sea urchin eggs, the $[Ca^{2+}]_i$ rise is caused by release of Ca^{2+} from the endoplasmic reticulum (ER) primarily through inositol 1,4,5-trisphosphate ($InsP_3$) receptors (Mohri et al., 1995; Lee et al., 1996) but also via ryanodine receptors (Galione et al., 1993; Lee et al., 1993). The $[Ca^{2+}]_i$ rise causes not only cortical granule exocytosis but also activation of cation channels responsible for phase 2 of the inward activation current (McCulloh and Chambers, 1991; Swann et al., 1992; Mohri et al., 1995). The activation potential and the FE formation serve as the early block and permanent block of polyspermy, respectively (Jaffe and Gould-Somero, 1985).

Interestingly, only a transient inward current corresponding to phase 1 is generated in about half of *L. variegatus* eggs, when membrane potential is held at levels more negative than –30 mV (Lynn et al., 1988). At these potentials, sperm entry into the ooplasm is prevented, although the mechanism is unknown (Lynn et al., 1988). The sperm that attached to the egg immediately detaches at potentials more negative than –80 mV, resulting in a sharp transient inward current (Lynn et al., 1988). Sperm-egg fusion is also inhibited by chemicals. Jaspisin (sodium (E)-5,6-dihydroxystyryl sulfate isolated from marine sponge), which has an inhibitory activity on hatching enzyme (a kind of metallo-endoproteinase), inhibits sperm-egg

membrane fusion in the sea urchin *Hemicentrotus pulcherrimus*, as demonstrated by lack of transfer of Hoechst 33342 (a DNA-staining fluorochrome) from the egg cytoplasm to the sperm nucleus (Ikegami et al., 1994).

Despite of the above information, simultaneous recordings of sperm-egg binding, membrane current and the $[Ca^{2+}]_i$ rise in a focal plane have not yet been performed. We conducted simultaneous recordings in *H. pulcherrimus* eggs using video image acquisition with infrared light, voltage clamp with a single microelectrode and Ca^{2+} imaging with confocal laser scanning microscopy. In addition, jaspisin at moderate concentrations was used to dissect various stages of sperm-egg fusion. The primary objective was to isolate from normal responses not only the earliest transient current but also the initial local $[Ca^{2+}]_i$ rise at the sperm attachment site, as a step to elucidate the mechanism of sperm-egg interaction leading to the Ca^{2+} wave.

MATERIALS AND METHODS

Gametes

Sea urchins *H. pulcherrimus* were collected from the coast of Seto Inland Sea near Hiroshima. Eggs were obtained by injecting 0.2-0.4 ml of 0.55 M KCl into the coelomic cavity. Whole testes removed from males were stored dry at 4°C. Gametes were used within 10 hours after shedding, only when over 90% of the eggs simultaneously elevated the symmetrical FE and cleaved regularly through the 4-cell stage. The jelly coats were removed immediately before use (for details, see Mohri et al., 1995). All experiments were carried out at 20-21°C using natural sea water (SW) passed through a membrane filter (0.22 μm), buffered with 10 mM tris(hydroxymethyl)-ethylaminopropane sulfonic acid (TAPS), and adjusted to pH 8.3 with NaOH.

Chemicals

The solution for injection of the Ca^{2+} indicator dye was composed of 2 mM Calcium Green dextran (M_r 1×10^4; Molecular Probes Inc., Eugene, OR), 140 mM KCl, 1 mM $MgCl_2$ and 5 mM Hepes, adjusted to pH 7.3 with KOH. Jaspisin was prepared from the marine sponge, *Jaspis* species, as previously described (Ikegami et al., 1994), and kept dry at 4°C. Jaspisin was dissolved in distilled water and diluted with SW immediately before use. Organic and inorganic chemicals were purchased from Sigma (St. Louis, MO) and Nakalai Tesque Inc. (Tokyo, Japan), respectively.

Membrane current recording

Membrane current was recorded by a single microelctrode voltage clamp system (CEZ-3100, Nihon Kohden, Tokyo) on a chart recorder. An egg was impaled with a glass microelectrode which was filled with 0.55 M KCl and had resistance of 20-30 MΩ. Membrane potential (V_m) was clamped at –20 mV. V_m before and after voltage clamp was checked by the current clamp mode. Details of the technique and procedure of voltage clamp have been described previously (Mohri et al., 1995).

Confocal microscopy

The spatial distribution of $[Ca^{2+}]_i$ rise was investigated with a confocal laser scanning microscope (CLSM; RCM 8000, Nikon, Tokyo) attached to an inverted microscope (TMD-300, Nikon). Fluorescence of Calcium Green dextran microinjected into the egg was excited by 488 nm argon laser with the minimum power required to provide an adequate signal-to-noise ratio. A 40× objective water immersion lens was used (Fluor 40, NA 1.15; Nikon). The optical section thickness was estimated to be 4.2 μm in the present experimental condition. Signals emitted over 510 nm were collected through a dichroic beam splitter at 510 nm to a photomultiplier and an image processor (MAX VIDEO). For fluorescence measurements, a background image (B) was first acquired in an egg-free optical field. Ca^{2+} images of the egg were acquired every second and each image was constituted by accumulating 16 frames to improve signal-to-noise ratio. Images were stored on an optical memory disc recorder (Model TQ-3800F, Panasonic Co., Tokyo).

Each fluorescence image of the egg during fertilization (F) was divided by an image just before sperm attachment (F_0), in a pixel-to-pixel manner as the ratio $R = (F-B)/(F_0-B)$. Processing was performed with custom macros on NIH Image (a public domain image processing software for the Macintosh computer). Processed images were expressed by pseudocolors in terms of R values. Rs in localized regions of the egg were taken as the average over a circle area of 24 pixels in diameter (egg diameter, ~195 pixels).

Bright-field images with infrared light (IR images)

Video-rate bright-field images were simultaneously obtained without interference to fluorescence images of CLSM, using infrared (IR) light, dichroic beam splitter at 650 nm, bandpass filter (735-770 nm) and IR camera (VC 820L, Tokyo Electronic Industry Co., Tokyo). IR images were recorded on an SVHS video cassette recorder (HR-VX11, Victor, Yokohama, Japan).

Experimental procedure

An experimental chamber was fashioned from a 35×10 mm plastic culture dish (Falcon #1008, Becton Dickinson, Lincoln, NJ). The bottom of the dish was cut out to make a hole of 20 mm in diameter, which was closed by a circular coverslip (30 mm in diameter) using dental wax. The cover slip was coated with 0.01% poly-L-lysine to facilitate adhesion of eggs. The chamber was mounted on the stage of the inverted microscope. About 50-100 de-jellied eggs were pipetted into the chamber filled with 4-5 ml SW containing jaspisin.

A Piezo micromanipulator (PMM-L, Prima Meat Packers, Tsuchiura, Japan) was used to insert an injection pipette into the egg rapidly with little damage. Calcium Green dextran was microinjected into eggs (1 to 2% of the egg volume) by a pressure microinjecter (IM-300, Narishige, Tokyo) which was controlled by an electronic stimulator (SEN-3301, Nihon Kohden). The pipette was withdrawn immediately after injection. The dye-injected egg was impaled by a microelectrode and voltage-clamped.

After starting simultaneous recordings of CLSM images and IR images as well as membrane current, insemination was conducted by gently pipetting 100 μl of diluted suspension of sperm (1-2 μl of dry sperm/40 ml SW) into the bath ~2 cm away from the experimental egg. The first sperm approaching the egg was detected and pursued by changing focus of IR images and CLSM was promptly adjusted at the focal plane on which the sperm attached to the egg surface, although exact focusing was not always possible. Recording was continued only when the sperm attached at the nearly equatorial egg surface. Elevation of the FE and other morphological changes were monitored by IR images. After the experiment, the egg's development was observed up to 2-cell stage.

Clocks of both CLSM and IR image acquisitions were synchronized with time difference less than 0.1 seconds. The time of the onset of a step inward current (I_{on}) was marked on the image processor by the observer. The time lag, if any, was within 0.5 seconds.

RESULTS

The resting membrane potential ranged between –20 and –60 mV. Eggs were voltage-clamped at –20 mV, at which potential level fertilization occurred probably without electrical block of sperm-egg fusion (Jaffe and Gould-Somero, 1985) or electrical

block of sperm entry into the egg (Lynn et al, 1988). This condition, however, allowed polyspermy to occur. To obtain monospermic fertilization or identify the spermatozoon responsible for changes in membrane current and $[Ca^{2+}]_i$, very low concentration of sperm suspension was added to the bath. Sperm entry and monospermic fertilization were identified later by the presence of the aster and regular cleavage. An abrupt step of inward current (I_{on}) occurred immediately after a spermatozoon attached to the egg (Fig. 1B). In the present paper, the time of I_{on} was defined as the zero time.

$[Ca^{2+}]_i$ increase and activation current in eggs at normal fertilization

The profile of the activation current and $[Ca^{2+}]_i$ increase in normal fertilization of *H. pulcherrimus* eggs is shown as the control. I_{on} occurred about 2 seconds after the attachment of the sperm to the egg surface (arrow sp in Fig. 1B). The amplitude of I_{on} was 0.15±0.01 nA (mean ± s.e.m., *n*=8), consistent with that in *L. variegatus* eggs (Lynn et al., 1988; Mohri et al., 1995). The inward current increased gradually and attained the major peak (I_p) at 45±4 seconds (*n*=8), while the time to the peak is 32-35 seconds in *L. variegatus* eggs (Mohri et al., 1995). The amplitude of I_p was 0.41±0.11 nA (*n*=8), which was much smaller than that in *L. variegatus* eggs. A smaller peak was often recognized prior to the major peak (Fig. 1B). After attaining I_p, the inward current declined gradually and shifted to an outward current at about 60 seconds (Fig. 1B). The outward current was 0.95±0.1 nA (*n*=6) in the maximal amplitude and persisted during current recording for several minutes.

The $[Ca^{2+}]_i$ began to increase at the site of sperm attachment (Fig. 2B) 6-10 seconds after I_{on}. On IR images, the sperm was still gyrating on the egg surface at the time of onset of the $[Ca^{2+}]_i$ rise and stopped moving around 22 seconds (24±3 seconds, *n*=8). The $[Ca^{2+}]_i$ rise propagated as a wave across the deep cytoplasm as well as the cortical cytoplasm (Fig. 2B-K), as demonstrated in other sea urchin species (Stricker et al., 1992; Shen and Buck, 1993; Gillot and Whitaker, 1994). Fig. 1A represents the time course of the $[Ca^{2+}]_i$ rise at four different sites: (1) sperm attachment site, (2) central site, (3) antipode site and (4) cortical site 90° against the sperm attachment site. At sites 1, 2 and 3, the $[Ca^{2+}]_i$ rise started at 8, 17 and 24 seconds after I_{on}, and attained the peak at 30, 43 and 56 seconds, respectively. The calculated propagation velocity of the wavefront was 5.6 μm/second (4.8±0.4 μm/second, *n*=4). The Ca^{2+} wave propagates at the similar velocity in the cortical and central ooplasm, as indicated by $[Ca^{2+}]_i$ rise at sites 4 and 2. At the cortical region (sites 1, 3 and 4), the $[Ca^{2+}]_i$ appeared to increase in two steps: the first rise and the second slower rise associated with a shoulder in-between (arrows in Fig. 1A). Precise analysis is necessary for the cortical $[Ca^{2+}]_i$ rise (see Discussion).

The inward current increased during propagation of the Ca^{2+} wave and attained I_p when the $[Ca^{2+}]_i$ rise in the antipode site reached about the half of its maximal peak (Fig. 1A,B). The outward current developed when the $[Ca^{2+}]_i$ rise reached the maximal peak in the whole egg.

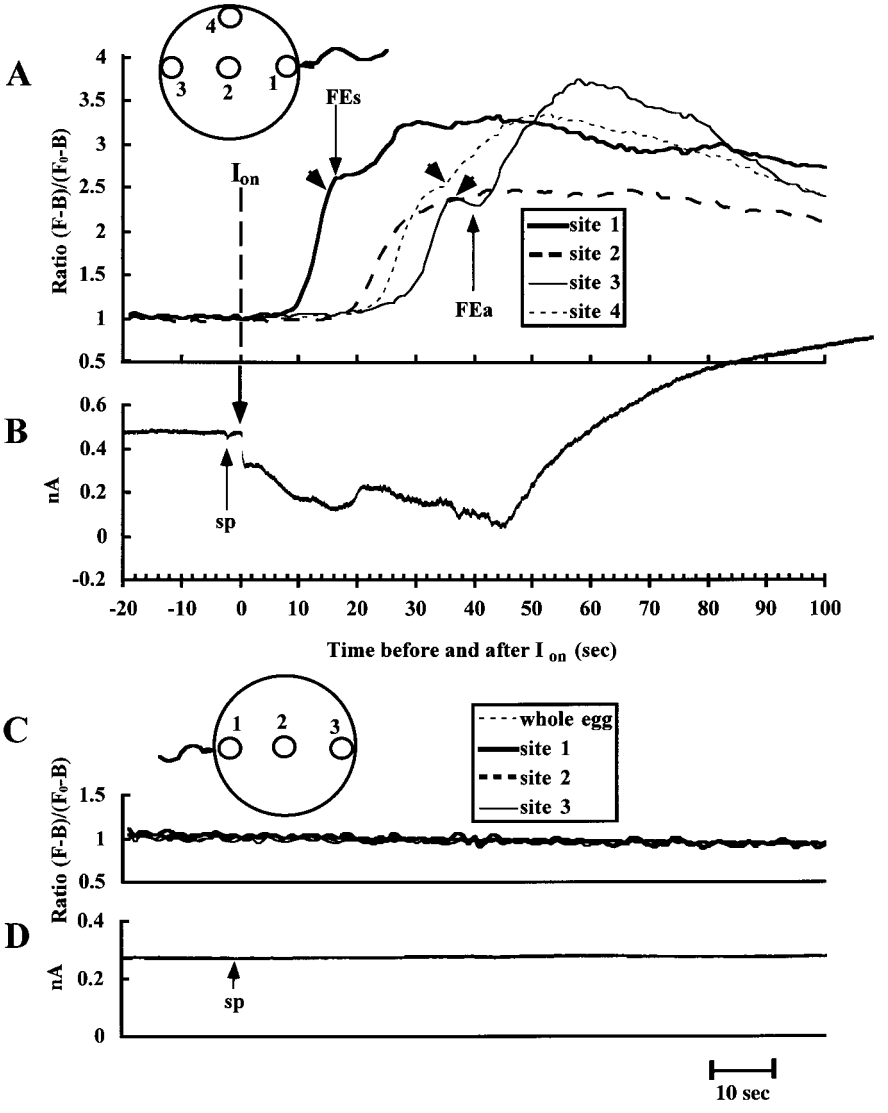

Fig. 1. Changes in $[Ca^{2+}]_i$ (A) and the membrane current (B) at normal fertilization of a *H. pulcherrimus* egg, and a complete block of the $[Ca^{2+}]_i$ rise (C) and a lack of the activation current (D) in an egg in the presence of 38 μM jaspisin. The time of I_{on} was taken as the zero time. The sites for fluorescence measurement and the corresponding lines for plotting are illustrated in the insets, in relation to the sperm attachment site. Inward membrane current is presented in the downward direction from the positive steady current to hold the membrane potential at –20 mV. Vertical arrows indicate the time as follows: sp, attachment of the sperm to the egg surface; FE_s and FE_a, the elevation of FE became visible at the sperm attachment site and the antipode site, respectively. The format of presentation is the same in Figs 1, 4 and 7. Arrowheads in A indicate the shoulder of the $[Ca^{2+}]_i$ rise at cortical regions.

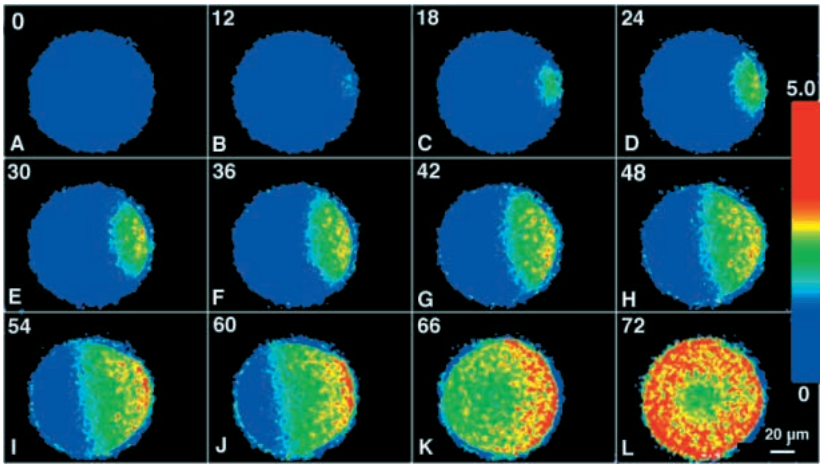

Fig. 2. Temporal ratio images (each image divided by an image just before I_{on}) showing the spatial distribution of the $[Ca^{2+}]_i$ rise at normal fertilization of the egg from which Fig. 1A,B were obtained. The optical section thickness was 4.2 μm. The number presented in each image is the time (in seconds) of acquisition after I_{on}. The method of obtaining images and the presentation are the same in Figs 2, 5 and 8. The color bar indicates ranges of fluorescence ratio values.

The FE was elevated, as the $[Ca^{2+}]_i$ rise propagated. Cortical reaction and a slight elevation of the FE at the sperm attachment site were first detected on IR video images at 18 seconds after I_{on} (Fig. 1A, arrow FEs), although not clearly shown on photographs. The period corresponded to the time when the $[Ca^{2+}]_i$ rise at site 1 reached the shoulder. The elevated FE became clearly visible at ~27 seconds (Fig. 3B), when the $[Ca^{2+}]_i$ rise at site 1 nearly attained the peak (Fig. 1A) and the Ca^{2+} wave had already propagated toward the central region (Fig. 2D,E). FE elevation was further enhanced at the sperm attachment site, while it propagated along the egg surface (Fig. 3C). The FE became visible at the antipode site at 39 seconds (Fig. 1A, arrow FEa), when the $[Ca^{2+}]_i$ rise at site 3 reached the shoulder. The egg of Figs 1-3 underwent monospermic fertilization: i.e. it cleaved normally and developed to 2-cell stage about 70 minutes after I_{on}.

No block or complete block of sperm-egg fusion by jaspisin

When eggs were inseminated in the presence of jaspisin at the concentration range between 16 and 34 μM, fertilization rate were variable with 70% of the eggs not fertilizing at all. 13 of 43 eggs exhibited an activation current and a $[Ca^{2+}]_i$ rise similar to those in the absence of jaspisin. The amplitudes of

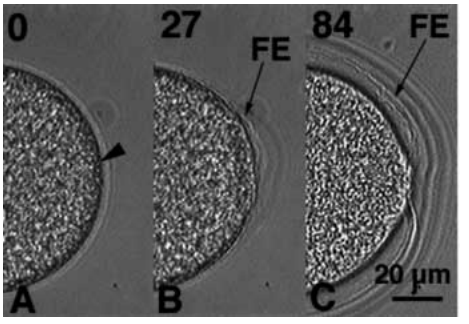

Fig. 3. Bright-field images of the egg for Figs 1A,B, 2. The number presented in each image is the time (in seconds) of acquisition after I_{on}. This presentation is the same in Figs 3, 6, 9. Arrowhead in A indicates the point of sperm attachment. The sperm head is slightly out of focus on photographs, although it was seen gyrating on video images. Arrow FE indicates the fertilization envelope.

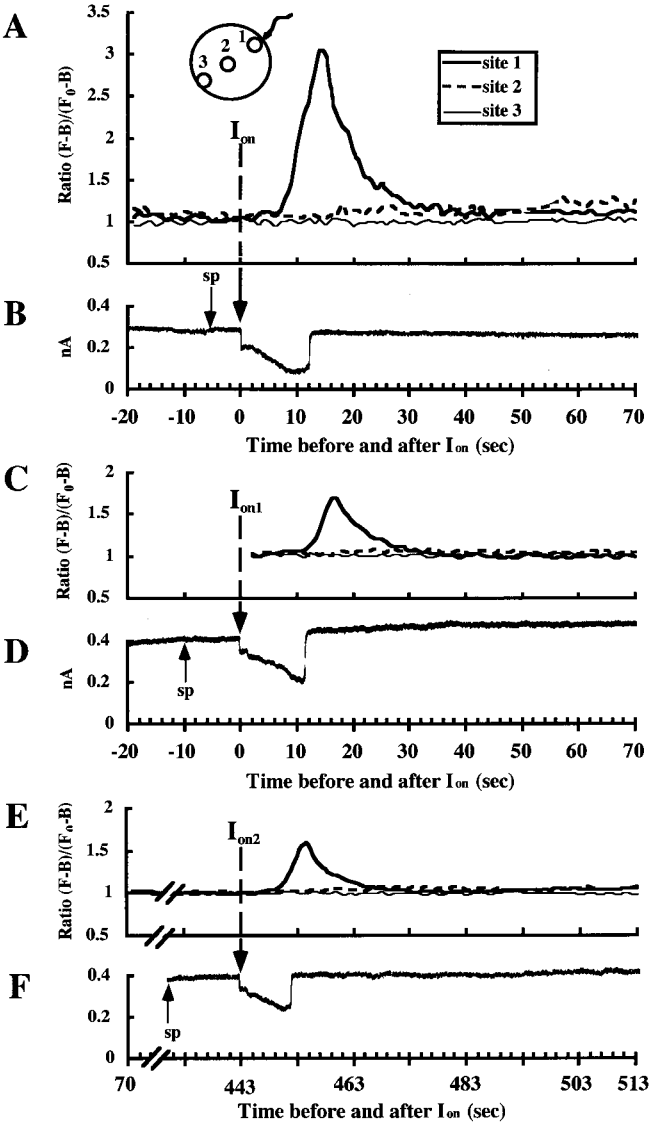

Fig. 4. Two examples of eggs which exhibited only transient $[Ca^{2+}]_i$ rises at the sperm attachment site (A,C,E) and transient inward currents (B,D,F) in the presence of 34 μM jaspisin. C-F were obtained from the same egg.

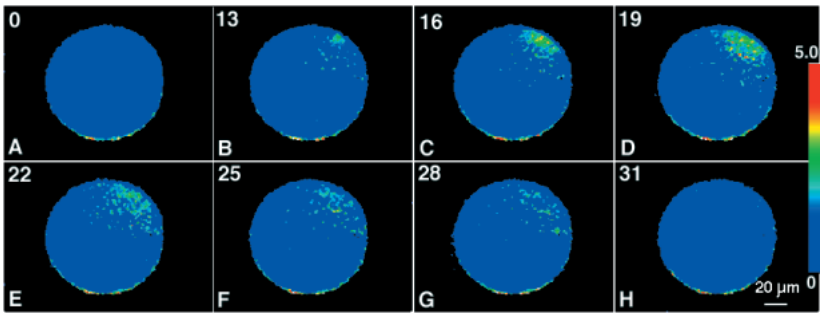

Fig. 5. Temporal ratio images showing the local $[Ca^{2+}]_i$ rise in the egg from which Fig 4A,B were obtained.

I_{on} and I_p were 0.14±0.01 nA and 0.56±0.07 nA (*n*=13), respectively. I_p occurred at 44±2 seconds. The magnitude and time course of the propagating $[Ca^{2+}]_i$ rise were also similar to those in the absence of jaspisin (not shown). The FE was elevated normally. Jaspisin appeared not to affect Ca^{2+}-dependent cortical vesicle exocytosis and the elevation of FE, unless sperm-egg fusion was prevented. When sperm entry was blocked by 16-34 μM jaspisin, eggs showed different aspects in the inward current and the $[Ca^{2+}]_i$ rise (see later sections).

No response was observed in 8/43 eggs inseminated in the presence of 16-34 μM jaspisin and 6/6 eggs at concentrations higher than 34 μM. I_{on} and any other change in membrane current did not occur (Fig. 1D), although many sperm attached to the egg. No $[Ca^{2+}]_i$ rise was detected in the entire egg (Fig. 1C), the FE did not elevate, there was no cleavage and no aster was observed. The failure of the fertilization response appeared to be caused by complete block of sperm-egg fusion by jaspisin (Ikegami et al., 1994).

Local $[Ca^{2+}]_i$ increase and transient inward current without sperm entry

In the presence of 16-34 μM jaspisin, the sperm that attached to the egg soon detached from the egg. Only a transient inward current but not an activation current was observed in 19/43 eggs (Fig. 4B,D,F). I_{on} occurred 5 seconds in Fig. 4B, 10 seconds in Fig. 4D, and 13 seconds in Fig. 4F after sperm attachment to the egg (14 seconds in another case). Thus, the sperm took substantially longer time to induce I_{on} compared with normal fertilization (~2 seconds). The amplitude of I_{on} was 0.09±0.01 nA (*n*=14), significantly smaller than that in normal fertilization ($P<0.01$). The inward current gradually increased after I_{on}. The current was, however, abruptly cut off (I_{off}) at 12 seconds in Fig. 4B,D and 9 seconds in Fig. 4F, and returned to the basal level. The mean duration between I_{on} and I_{off} was 13.5±1.3 seconds (*n*=14). In 10/14 eggs, similar transient inward currents occurred repetitively in the same egg (2 to 6 transient currents during the recording of several minutes). The transient inward current appears to be comparable to that seen in inseminated *L. variegatus* eggs at potentials more negative than –30 mV (Lynn et al., 1988; Chambers, 1989).

In the eggs that exhibited the transient inward current alone, the transient $[Ca^{2+}]_i$ rise was generated, not in a wave but restricted at the sperm attachment site (Figs 4A,C,E, 5). Fig. 4C,E shows two transient $[Ca^{2+}]_i$ rises in the same egg. In Fig. 4A,C,E the $[Ca^{2+}]_i$ began to increase at 7, 10 and 6 seconds after I_{on}, preceded by the increase of the inward current. However, the increasing $[Ca^{2+}]_i$ was abruptly reduced, forming a peak. The time of the peak $[Ca^{2+}]_i$ was 14 seconds (Fig. 4A), 16 seconds (Fig. 4C) or 12 seconds (Fig. 4E): that is, 2-4 seconds after I_{off}, respectively. $[Ca^{2+}]_i$ returned to the basal level at 25 to 35 seconds. The total duration of the transient $[Ca^{2+}]_i$ rise was 22±3 seconds (n=9). The transient $[Ca^{2+}]_i$ rise was restricted to the vicinity of the sperm attachment site, within 15 μm from the sperm attachment point on the focal plane (Fig. 5C,D).

I_{off} is thought to be caused by detachment of the sperm from the egg surface (Lynn et al., 1988; Chambers, 1989). On IR images, the sperm appeared gyrating on the egg surface at the time of I_{off} and the detachment of the sperm was recognized a little later. Fig. 6 (the same egg as Figs 4A,B, 5) shows that the sperm head seen on the egg surface at 0 and 5 seconds after I_{on} (Fig. 6A,B) was slightly detached from the egg surface at 15 seconds (Fig. 6C) and clearly separated at 41 seconds (Fig. 6D). No visible FE formation was recognized at the site of sperm attachment (Fig. 6D).

Delayed Ca^{2+} wave and activation current without sperm entry

In 3/43 eggs inseminated in the presence of 16-34 μM jaspisin, the transient inward current and the local $[Ca^{2+}]_i$ rise were followed by the activation current and the Ca^{2+} wave after a substantial delay, although sperm entry was prevented. In Fig. 7B, I_{on} appeared 3 seconds after the sperm attachment and I_{off} occurred at 12 seconds after I_{on}. A local $[Ca^{2+}]_i$ rise began 7 seconds after I_{on} (Fig. 7A; see Figure Legends for a transient decline of fluorescence ratio indicated by arrows to be an artifact caused by changing focus). The increasing $[Ca^{2+}]_i$ was abruptly reduced, forming a peak at 14 seconds (2 seconds after I_{off}) (Fig. 7A). The $[Ca^{2+}]_i$ rise was localized at the sperm attachment site (Fig. 8B-G). This is thought to correspond to the transient $[Ca^{2+}]_i$ rise described in the previous section. The sperm head was in contact with the egg at 15 seconds (Fig.

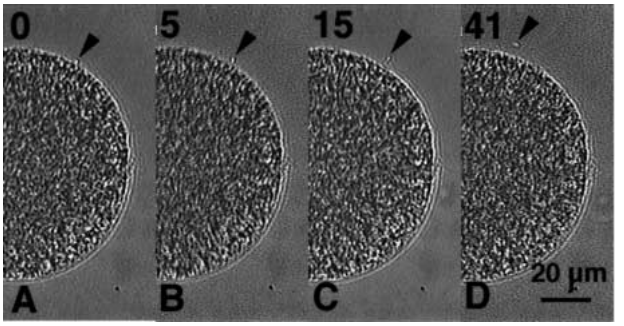

Fig. 6. Bright-field images of the egg for Figs 4A,B, 5. Arrowhead indicates the sperm head.

9B), but was about 10 μm away from the egg surface at 20 seconds (Fig. 9C). The FE was not yet visible at that time. Thus, it was unlikely that the FE dispelled the sperm, although the sperm detachment could be affected by FE elevation at the electron microscopic level.

In Fig. 7A, the $[Ca^{2+}]_i$ increase started again at 22 seconds at the sperm attachment site, although the sperm had already detached from the egg surface (Fig. 9C). The $[Ca^{2+}]_i$ rise at the site close to the sperm attachment site started at 25 seconds without a preceding transient $[Ca^{2+}]_i$ rise (Fig. 7A, site 4), and then a Ca^{2+} wave was generated (Fig. 8H-L). The $[Ca^{2+}]_i$ rise at the antipode site began at 42 seconds (Fig. 7A, site 3). The velocity of the wavefront was approximately 4.5 μm/second, similar to that in normal fertilization.

The inward current appeared again at about 27 seconds after I_{on} and increased slowly (Fig. 7B), corresponding to the delayed start and slow propagation of the Ca^{2+} wave. The inward current was soon replaced by the outward current, as in normal fertilization. The delayed activation current seems to be comparable to modified activation which is seen when sperm entry is prevented by hyperpolarization of membrane potential (Lynn et al., 1988).

Elevation of the FE at the sperm attachment site was detected at about 40 seconds after I_{on} (Fig. 7A, arrow FEs). In the egg from which Figs 7, 8 were obtained, the FE was only partially elevated near the sperm attachment site, while fully elevated in other area (Fig. 9E). The egg shrank near the sperm attachment site (Fig. 9D), so that calculation of fluorescence ratio at site 1 of Fig. 7A became impossible (see the 4 o'clock position of the egg in Fig. 8K-L; see the interruption of curve 1 in Fig. 7A). Neither cleavage nor an aster was observed in this egg, indicating no sperm entry.

DISCUSSION

The present study demonstrated the sperm-induced earliest transient current and local $[Ca^{2+}]_i$ rise in *H. pulcherrimus* eggs, isolated from normal responses by the condition in which temporal sperm-egg fusion was produced by jaspisin. The transition of this current to the activation current and the $[Ca^{2+}]_i$ rise to the Ca^{2+} wave was clearly shown by a certain time lag in-between. The $[Ca^{2+}]_i$ rise localized at the sperm attachment site was first recorded by CLSM simultaneously with the observation of sperm-egg binding and membrane current. The present study provides some clues for further studies to elucidate the mechanism of fertilization.

Earliest membrane current

The earliest event, I_{on}, occurred 2 seconds after sperm-egg contact in normal fertilization. Sperm-egg membrane fusion may be formed at the time of I_{on}, since I_{on} is localized at the sperm attachment site as recorded with a patch electrode and the electrical coupling between the sperm and egg is detected at I_{on} by membrane capacitance measurements (McCulloh and Chambers, 1991, 1992). The step inward current began to increase 2 to 3 seconds after I_{on}, preceding the initiation of the $[Ca^{2+}]_i$ rise at the sperm attachment site which was recognized 6 to 10 seconds after I_{on}. The early inward current is, therefore, thought not to be the consequence of the $[Ca^{2+}]_i$ rise. The increasing inward current was abruptly cut off at 9-15 seconds after I_{on} by jaspisin. Based on IR image observation, I_{off} is thought to be caused by detachment of the sperm from the egg.

Jaspisin inhibits sperm-egg membrane fusion in *H. pulcherrimus*, but does not inhibit endoplasmic membrane fusion upon acrosome reaction of the sperm and cortical reaction of the egg (Ikegami et al., 1994). Jaspisin has the activity of inhibiting the sea urchin hatching enzyme (Ikegami et al., 1994), a kind of metallo-endoproteinase. Evidence has suggested the involvement of Zn^{2+}-dependent endoproteinase in gamete fusion of the sea urchin (Farach et al., 1987; Roe et al., 1988; Lennarz and Strittmatter, 1991). Jaspisin is likely to inhibit sperm-egg membrane fusion by its inhibitory action on a metallo-endoproteinase. Modification of surface proteins such as adhesion molecules or sperm receptors (Foltz and Lennarz, 1992) by the endoproteinase may facilitate membrane binding and fusion. Such protein(s) might be affected by membrane hyperpolarization which also causes detachment of the sperm. The sperm was gyrating on the egg surface for 20

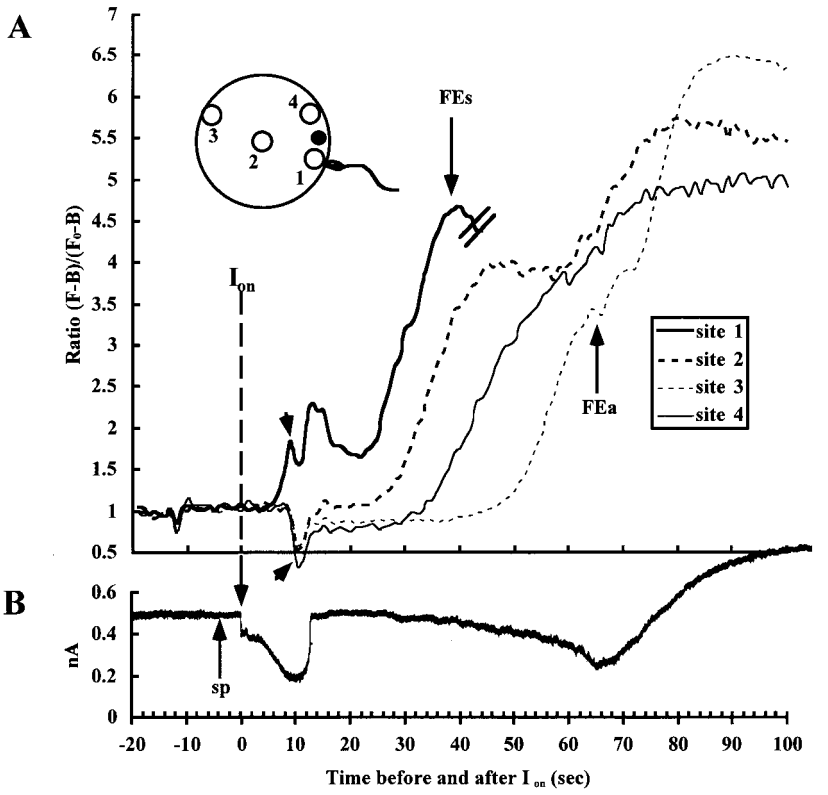

Fig. 7. Local $[Ca^{2+}]_i$ rise followed by the delayed Ca^{2+} wave (A) and transient inward current followed by the delayed activation current (B), induced without sperm entry in the presence of 32 μM jaspisin. Fluorescence ratio at the sperm attachment site became zero because of deformation of the egg, so that the curve was interrupted in A. Transient decrease in the fluorescence ratio at all sites (indicated by arrowheads) is an artifact caused by changing focus of CLSM to look for another sperm. The focus was returned to the focal plane of the sperm head responsible for generating the inward current and the $[Ca^{2+}]_i$ rise and was fixed there.

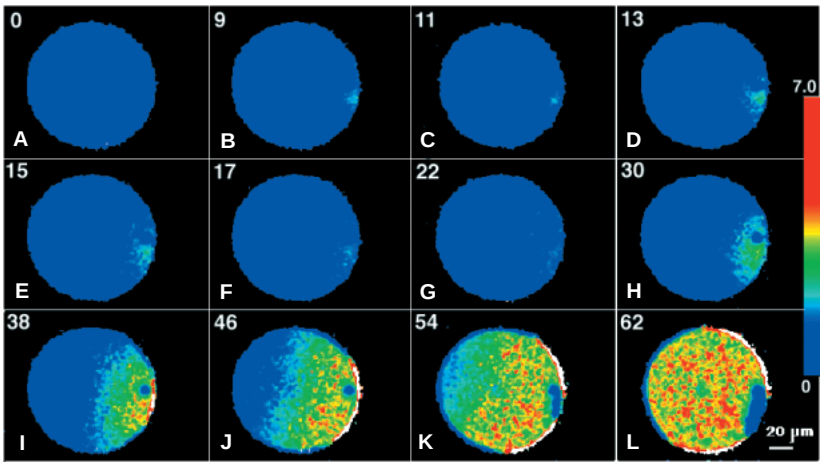

Fig. 8. Temporal ratio images showing the spatial distribution of the $[Ca^{2+}]_i$ rise in the egg for Fig. 7. The small blue spot seen at the 3 o'clock position in H to L was due to a vesicle which was formed by micropipette manipulation for injection of Calcium Green. The blue area at about 4 o'clock position in K and L corresponds to the egg deformation.

seconds or more even in normal fertilization, suggesting that gamete fusion may not be stable during this period in *H. pulcherrimus.* In the presence of jaspisin, the sperm took 5 to 14 seconds instead of 2 seconds in normal fertilization to induce I_{on} of the transient inward current after attachment to the egg, and the amplitude of I_{on} was significantly smaller than that in normal fertilization, suggesting some difficulty in forming membrane fusion. Such sperm are likely to readily detach from the egg, resulting in I_{off}. In future studies, it is a central subject to identify the putative surface protein related to metallo-endoproteinase and elucidate its function.

Local $[Ca^{2+}]_i$ rise

$[Ca^{2+}]_i$ rise began at the sperm attachment site 6 to 10 seconds after I_{on}, irrespective of the presence of jaspisin, unless gamete fusion was completely blocked. The $[Ca^{2+}]_i$ rise was localized at the vicinity (10-15 μm) of the sperm attachment point. The increasing $[Ca^{2+}]_i$ suddenly underwent a decline 1-3 seconds after I_{off} in the presence of jaspisin. The $[Ca^{2+}]_i$ rise seems to be turned off by sperm detachment. The transient local $[Ca^{2+}]_i$ rise recorded by the present experiments is the key phenomenon to elucidate the first stimulation by the sperm onto the egg. The critical points to be revealed in the next experiments will be whether the local $[Ca^{2+}]_i$ rise is due to either Ca^{2+} influx from outside of the egg or Ca^{2+} release from intracellular stores and whether it is coupled with the transient inward current.

As to the initiation of the $[Ca^{2+}]_i$ rise, so far three hypotheses have been proposed (Créton and Jaffe, 1995): (1) the sperm contact hypothesis (Foltz and Shilling, 1993; Jaffe, 1996), (2) the sperm content hypothesis (Swann, 1993; Whitaker and Swann, 1993) and (3) the sperm conduit hypothesis (Jaffe, 1990). An idea is that sperm-egg contact involving ligand-receptor binding causes the production of $InsP_3$ leading to Ca^{2+} release, or that it causes opening of cation-permeable channels that mediate an increasing inward current involving Ca^{2+} influx and, thereby, a small delayed local $[Ca^{2+}]_i$ rise. The problem in confirming Ca^{2+} influx is that gamete fusion is prevented in Ca^{2+}-free medium. Créton and Jaffe (1995) showed that activation of *L. variegatus* eggs is inhibited by adding lanthanum or by reducing external Ca^{2+} with a Ca^{2+} chelator BAPTA 5 to 20 seconds after sperm-egg binding and claimed that Ca^{2+} influx is needed during the latent period to induce the Ca^{2+} wave. Their hypothesis is that Ca^{2+} influx is brought from the sperm's acrosomal process to the egg's ER through the fusion pore and that Ca^{2+} release is initiated by overloading of the ER with Ca^{2+}. In this respect, it is a primary prerequisite to determine whether the local $[Ca^{2+}]_i$ rise is due to Ca^{2+} influx.

The sperm content hypothesis predicts a cytosolic sperm factor, which is transferred to the ooplasm through the fusion pore and induces Ca^{2+} release from the ER (Swann, 1993; Whitaker and Swann, 1993). Such a substance has not yet been identified, although a Ca^{2+} oscillation-inducing protein, oscillin, has been purified from the hamster sperm (Parrington et al., 1996). Diffusion of the sperm factor into the ooplasm could account for the time lag between I_{on} and the $[Ca^{2+}]_i$ rise. The transient $[Ca^{2+}]_i$ rise in the presence of jaspisin could be explained by the presence of an insufficient amount of the diffusing messenger to induce a Ca^{2+} wave, because of the interruption of sperm-egg fusion. The transient $[Ca^{2+}]_i$ rise continued even after I_{off} and the spatial extent of $[Ca^{2+}]_i$ rise was not exactly restricted to the small point of the sperm attachment point. These findings suggest a regenerative

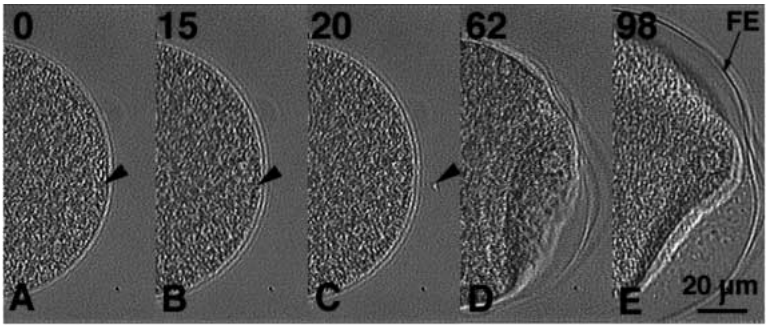

Fig. 9. Bright-field images of the egg for Figs 7, 8. The sperm head is slightly out of focus in A and B, but just in focus in C (arrowheads).

component in the transient $[Ca^{2+}]_i$ rise, unlike the direct consequence of Ca^{2+} influx through sperm-egg fusion point.

The present study still does not give any evidence supporting exclusively one hypothesis. An interesting finding is that the Ca^{2+} wave can be induced after the sperm detached from the egg and the initial local $[Ca^{2+}]_i$ rise had declined (Figs 7A, 8, 9C). This suggests a delayed augmenting mechanism in Ca^{2+} release from the ER. The hamster sperm factor augments the sensitivity of Ca^{2+} release to Ca^{2+} (Ca^{2+}-induced Ca^{2+} release, CICR) (Swann, 1993). CICR mechanism may develop through the aid of the sperm factor with a time lag, even when the preceding local $[Ca^{2+}]_i$ rise declines. The idea of loading-dependent Ca^{2+} release could also account for the delayed onset of the Ca^{2+} wave.

Ca^{2+} wave and activation current

The Ca^{2+} wave propagated in the deep cytoplasm as well as the cortical region at a similar velocity. The $[Ca^{2+}]_i$ in the cortical region appeared to increase in two steps. The FE became visible at about the time when the $[Ca^{2+}]_i$ rise reached a shoulder. The two-step $[Ca^{2+}]_i$ rise may be an artifact of fluorescence intensity increase caused by changes in the thickness of the egg and/or the redistribution of the intracellular dye during cortical reaction, fertilization envelope elevation and contraction-like movement of the egg. Therefore, precise analysis of the cortical $[Ca^{2+}]_i$ rise is necessary using two dyes such as Calcium Green and Fura Red or a dye with two emission lights such as indo-1 for ratio imaging.

The activation current is the consequence of the $[Ca^{2+}]_i$ rise in the egg's cortex. The inward current attained the peak, when the Ca^{2+} wave reached the antipode site. The increasing inward current is thought to be partly due to the increase of the cortical area where the $[Ca^{2+}]_i$ rise took place. The slower increase and smaller amplitude of the inward current in comparison with that of *L. variegatus* eggs are probably due to coexistence of the outward current, possibly K^+ current, which becomes dominant at about 60 seconds after I_{on}. The outward current develops during the early stage of egg activation in *H. pulcherrimus* eggs, when compared with other sea urchin species (Steinhardt et al., 1972; Lynn et al., 1988).

Thus, the present method comprising simultaneous recordings of bright-field images, confocal Ca^{2+} images and membrane current provides useful information on the sequential relationship of early events at fertilization.

We thank Dr R. Deguchi for useful discussion and Mrs Y. Nakajima for technical assistance.

REFERENCES

Chambers, E. L. (1989). Fertilization in voltage clamped sea urchin eggs. In *Mechanisms of Egg Activation* . (ed. R. Nuccitelli, G. N. Cherr and W. H. Clark Jr), pp. 1-18. New York: Plenum Press.

Créton, R. and Jaffe, L. F. (1995). Role of calcium influx during the latent period in sea urchin fertilization. *Dev. Growth Differ.* **37**, 703-709.

Epel, D. (1978). Mechanisms of activation of sperm and egg during fertilization of sea urchin gametes. *Curr. Top. Dev. Biol.* **12**, 185-261.

Farach, H. A., Mundy, D. I., Strittmatter, W. J. and Lennarz, W. J. (1987). Evidence for the involvement of metalloendoproteinases in the acrosome reaction in sea urchin sperm. *J. Biol. Chem.* **262**, 5483-5487.

Foltz, K. R. and Lennarz, W. J. (1992). Identification of the sea urchin egg receptor for sperm using an antiserum raised against a fragment of its extracellular domain. *J. Cell Biol*. **116**, 647-658.

Foltz, K. R. and Shilling, F. M. (1993). Receptor-mediated signal transduction and egg activation. *Zygote* **1**, 276-279.

Galione, A., McDougall, A., Busa, W. B., Willmott, N., Gillot, I. and Whitaker, M. (1993). Redundant mechanisms of calcium-induced calcium release underlying calcium waves during fertilization of sea urchin eggs. *Science* **261**, 348-352.

Gillot, and Whitaker, M. (1994). Calcium signals in and around the nucleus in sea urchin eggs. *Cell Calcium* **16**, 269-278.

Ikegami, S., Kobayashi, H., Myotoishi, Y., Ohta, S. and Kato, K. H. (1994). Selective inhibition of exoplasmic membrane fusion in echinoderm gametes with jaspisin, a novel antihatching substance isolated from marine sponge. *J. Biol. Chem.* **269**, 23262-23267.

Jaffe, L. A. (1996). Egg membranes during fertilization. In *Molecular Biology of Membrane Transport Disorders.* (ed. S. G. Schultz et al.), pp. 367-378, New York: Prenum Press.

Jaffe, L. A. and Gould-Somero, M. (1985). Polyspermy preventing mechanisms. In *Biology of Fertilization.* (ed. C.B. Metz and A. Monroy), pp. 223-243. New York: Academic Press.

Jaffe, L. F. (1985). The role of calcium explosions, waves and pulses in activating eggs. In *Biology of Fertilization.* (ed. C.B. Metz and A. Monroy), pp. 127-165. New York: Academic Press.

Jaffe, L.F. (1990). The roles of intermembrane calcium in polarizing and activating eggs. In *Mechanisms of Fertilization.* (ed. B. Dale), pp. 389-418. Berlin: Springer Verlag.

Lee, H. C., Aarhus, R. and Walseth, T. F. (1993). Calcium mobilization by dual receptors during fertilization of sea urchin eggs. *Science* **261**, 352-355.

Lee, S-J, Christenson, L., Martin, T. and Shen, S. (1996). The cyclic GMP-mediated calcium release pathway in sea urchin eggs is not required for the rise in calcium during fertilization. *Dev. Biol.* **180**, 324-335.

Lennarz, W. J. and Strittmatter, W. J. (1991). Cellular functions of mettallo-endoproteinases. *Biochim. Biophys. Acta* **1071**, 149-158.

Lynn, J. W., McCulloh, D. H. and Chambers, E. L. (1988). Voltage clamp studies of fertilization in sea urchin eggs. II. Current patterns in relation to sperm entry, monospermy, nonespermy, and activation. *Dev. Biol.* **128**, 305-323.

McCulloh, D. H. and Chambers, E. L. (1991). A localized zone of increased conductance progresses over the surface of the sea urchin egg during fertilization. *J. Gen. Physiol.* **97**, 579-604.

McCulloh, D. H. and Chambers, E. L. (1992). Fusion of membranes during fertilization. Increases of the sea urchin egg's membrane capacitance and membrane conductance at the site of contact of sperm. *J. Gen. Physiol.* **99**, 137-175.

Mohri, T., Ivonnet, P. I. and Chambers, E. L. (1995). Effect on sperm-induced activation current and increase of cytosolic Ca^{2+} by agents that modify the mobilization of $[Ca^{2+}]_i$. I. Heparin and pentosan polysulfate. *Dev. Biol.* **172,** 139-157.

Parrington, J., Swann, K., Shevchenko, V. I., Sesay, A. K. and Lai, A. F. (1996). Calcium oscillations in mammalian eggs triggered by a soluble sperm protein. *Nature* **379**, 364-368.

Roe, J. L., Farach, H. A., Jr., Strittmatter, W. J. and Lennarz, W. J. (1988). Evidence for involvement of metalloendoproteinases in step in sea urchin gamete fusion. *J. Cell Biol.* **107**, 539-544.

Shen, S. S. and Buck, W. R. (1993). Sources of calcium in sea urchin eggs during the fertilization responses. *Dev. Biol.* **157,** 157-169.

Steinhardt, A. R., Shen, S., and Mazia, D. (1972). Membrane potential, membrane resistance and energy requirement for the development of potassium conductance in the fertilization reaction of echinoderm eggs. *Exp. Cell Res.* **72**, 195-203.

Stricker, S. A., Centonze, V. E., Paddock, S. W. and Schatten, G. (1992). Confocal microscopy of fertilization-induced calcium dynamics in sea urchin eggs. *Dev. Biol.* **149,** 370-380.

Swann, K. (1993). The soluble sperm oscillogen hypothesis. *Zygote*. **1,** 273-276.

Swann, K., McCulloh, D. H., McDougall, A., Chambers, E. L. and Whitaker, M. (1992). Sperm-induced currents at fertilization in sea urchin eggs injected with EGTA and neomycin. *Dev. Biol.* **151**, 552-560

Whitaker, M. and Swann, K. (1993). Lighting the fuse at fertilization. *Development* **117**, 1-12.